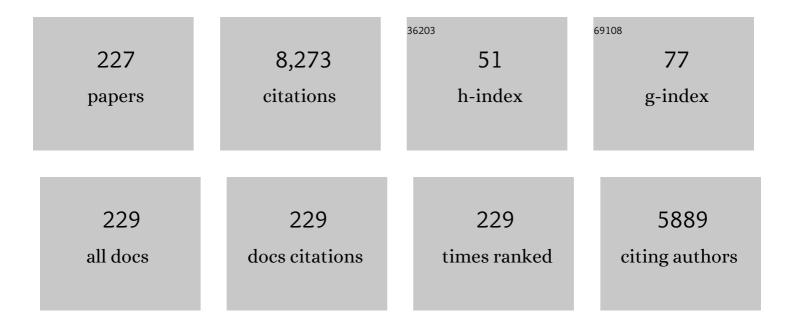
List of Publications by Year in descending order

Source: https://exaly.com/author-pdf/3490188/publications.pdf Version: 2024-02-01



#	Article	IF	CITATIONS
1	Mechanical properties and machining performance of Ti1â^'xAlxN-coated cutting tools. Surface and Coatings Technology, 2005, 191, 384-392.	2.2	475
2	Thermal stability of arc evaporated high aluminum-content Ti1â^'xAlxN thin films. Journal of Vacuum Science and Technology A: Vacuum, Surfaces and Films, 2002, 20, 1815-1823.	0.9	314
3	Nanoindentation studies of singleâ€crystal (001)â€, (011)â€, and (111)â€oriented TiN layers on MgO. Journal of Applied Physics, 1996, 80, 6725-6733.	1.1	239
4	Evolution of the residual stress state in a duplex stainless steel during loading. Acta Materialia, 1999, 47, 2669-2684.	3.8	163
5	Nanostructure formation during deposition of TiNâ^•SiNx nanomultilayer films by reactive dual magnetron sputtering. Journal of Applied Physics, 2005, 97, 114327.	1.1	145
6	Interface structure in superhard TiN-SiN nanolaminates and nanocomposites: Film growth experiments and ab initiocalculations. Physical Review B, 2007, 75, .	1.1	142
7	xmins:mmi="http://www.w3.org/1998/Math/Math/Math/M_display="inline"> <mmi:msub><mmi:mrow /&gt;<mmi:mrow><mmi:mn>0.5</mmi:mn></mmi:mrow></mmi:mrow </mmi:msub> Al <mmi:math xmlns:mml="http://www.w3.org/1998/Math/MathML" display="inline"&gt;<mmi:msub><mmi:mrow /&gt;<mmi:mrow><mmi:mn>0.5</mmi:mn></mmi:mrow></mmi:mrow </mmi:msub><td>1.1</td><td>125</td></mmi:math 	1.1	125
8	elastic constants on size and shape of the supercell model and their convergence. Physical Review 8, Growth of single-crystal CrN on MgO(001): Effects of low-energy ion-irradiation on surface morphological evolution and physical properties. Journal of Applied Physics, 2002, 91, 3589-3597.	1.1	117
9	Significant elastic anisotropy in Ti1â~'xAlxN alloys. Applied Physics Letters, 2010, 97, .	1.5	107
10	Microstructure, stress and mechanical properties of arc-evaporated Cr–C–N coatings. Thin Solid Films, 2001, 385, 190-197.	0.8	106
11	Strain and texture analysis of coatings using high-energy x-rays. Journal of Applied Physics, 2003, 94, 697-702.	1.1	103
12	Strain evolution during spinodal decomposition of TiAlN thin films. Thin Solid Films, 2012, 520, 5542-5549.	0.8	101
13	Improving thermal stability of hard coating films via a concept of multicomponent alloying. Applied Physics Letters, 2011, 99, .	1.5	95
14	Microstructure and mechanical behavior of arc-evaporated Cr–N coatings. Surface and Coatings Technology, 1999, 114, 39-51.	2.2	94
15	Microwave assisted combustion synthesis of nanocrystalline yttria and its powder characteristics. Powder Technology, 2009, 191, 309-314.	2.1	92
16	Epitaxial NaCl structure δ-TaNx(001): Electronic transport properties, elastic modulus, and hardness versus N/Ta ratio. Journal of Applied Physics, 2001, 90, 2879-2885.	1.1	88
17	Thermally enhanced mechanical properties of arc evaporated Ti0.34Al0.66N/TiN multilayer coatings. Journal of Applied Physics, 2010, 108, .	1.1	86
18	Layer formation by resputtering in Ti–Si–C hard coatings during large scale cathodic arc deposition. Surface and Coatings Technology, 2011, 205, 3923-3930.	2.2	83

#	Article	IF	CITATIONS
19	Combustion synthesis of Y2O3 and Yb–Y2O3. Journal of Materials Processing Technology, 2008, 208, 415-422.	3.1	82
20	Load sharing between austenite and ferrite in a duplex stainless steel during cyclic loading. Metallurgical and Materials Transactions A: Physical Metallurgy and Materials Science, 2000, 31, 1557-1570.	1.1	81
21	Immobilization of lipase from Mucor miehei and Rhizopus oryzae into mesoporous silica—The effect of varied particle size and morphology. Colloids and Surfaces B: Biointerfaces, 2012, 100, 22-30.	2.5	81
22	Phase Stability and Elasticity of TiAlN. Materials, 2011, 4, 1599-1618.	1.3	80
23	Mechanical and thermal stability of TiN/NbN superlattice thin films. Surface and Coatings Technology, 2000, 133-134, 227-233.	2.2	79
24	Thermal stability, microstructure and mechanical properties of Ti1â^²xZrxN thin films. Thin Solid Films, 2008, 516, 6421-6431.	0.8	76
25	Thermal decomposition products in arc evaporated TiAlN/TiN multilayers. Applied Physics Letters, 2008, 93, .	1.5	74
26	Cluster formation at the Si/liquid interface in Sr and Na modified Al–Si alloys. Scripta Materialia, 2016, 117, 16-19.	2.6	74
27	Stepwise transformation behavior of the strain-induced martensitic transformation in a metastable stainless steel. Scripta Materialia, 2007, 56, 213-216.	2.6	72
28	Rapid Synthesis of SBA-15 Rods with Variable Lengths, Widths, and Tunable Large Pores. Langmuir, 2011, 27, 4994-4999.	1.6	72
29	Epitaxial stabilization of cubic-SiNx in TiNâ^•SiNx multilayers. Applied Physics Letters, 2006, 88, 191902.	1.5	71
30	Load Partitioning and Strain-Induced Martensite Formation during Tensile Loading of a Metastable Austenitic Stainless Steel. Metallurgical and Materials Transactions A: Physical Metallurgy and Materials Science, 2009, 40, 1039-1048.	1.1	71
31	In situ X-ray scattering study of the cubic to hexagonal transformation of AlN in Ti1â^'xAlxN. Acta Materialia, 2014, 73, 205-214.	3.8	71
32	Fabrication of transparent yttria by HIP and the glass-encapsulation method. Journal of the European Ceramic Society, 2009, 29, 311-316.	2.8	69
33	Pressure enhancement of the isostructural cubic decomposition in Ti1â^xAlxN. Applied Physics Letters, 2009, 95, .	1.5	67
34	Machining performance and decomposition of TiAlN/TiN multilayer coated metal cutting inserts. Surface and Coatings Technology, 2011, 205, 4005-4010.	2.2	67
35	Growth and physical properties of epitaxial metastable cubic TaN(001). Applied Physics Letters, 1999, 75, 3808-3810.	1.5	65
36	Characterization of the Induced Plastic Zone in a Single Crystal TiN(001) Film by Nanoindentation and Transmission Electron Microscopy. Journal of Materials Research, 1997, 12, 2134-2142.	1.2	64

#	Article	IF	CITATIONS
37	X-ray photoelectron spectroscopy studies of Ti1-Al N (0â€^â‰≇€^xâ€^â‰≇€^0.83) high-temperature oxidation: crucial role of Al concentration. Surface and Coatings Technology, 2019, 374, 923-934.	The <sub>2.2</sub>	64
38	Spinodal decomposition of Ti0.33Al0.67N thin films studied by atom probe tomography. Thin Solid Films, 2012, 520, 4362-4368.	0.8	63
39	Microstructure evolution during the isostructural decomposition of TiAlN <i>—</i> A combined <i>in-situ</i> small angle x-ray scattering and phase field study. Journal of Applied Physics, 2013, 113, .	1.1	63
40	Shape engineering vs organic modification of inorganic nanoparticles as a tool for enhancing cellular internalization. Nanoscale Research Letters, 2012, 7, 358.	3.1	61
41	Grinding Effects on Surface Integrity and Mechanical Strength of WC-Co Cemented Carbides. Procedia CIRP, 2014, 13, 257-263.	1.0	61
42	Magnetron sputtered W–C films with C60 as carbon source. Thin Solid Films, 2003, 444, 29-37.	0.8	60
43	Lattice Vibrations Change the Solid Solubility of an Alloy at High Temperatures. Physical Review Letters, 2016, 117, 205502.	2.9	60
44	Microstructural evolution during tempering of arc-evaporated Cr–N coatings. Journal of Vacuum Science and Technology A: Vacuum, Surfaces and Films, 2000, 18, 121-130.	0.9	59
45	<i>In situ</i> small-angle x-ray scattering study of nanostructure evolution during decomposition of arc evaporated TiAlN coatings. Applied Physics Letters, 2009, 94, .	1.5	59
46	Effects of Ti alloying of AlCrN coatings on thermal stability and oxidation resistance. Thin Solid Films, 2013, 534, 394-402.	0.8	59
47	Comparison of segregations formed in unmodified and Sr-modified Al–Si alloys studied by atom probe tomography and transmission electron microscopy. Journal of Alloys and Compounds, 2014, 611, 410-421.	2.8	59
48	The effects on pore size and particle morphology of heptane additions to the synthesis of mesoporous silica SBA-15. Microporous and Mesoporous Materials, 2010, 133, 66-74.	2.2	58
49	Influence of elastic and plastic anisotropy on the flow behavior in a duplex stainless steel. Metallurgical and Materials Transactions A: Physical Metallurgy and Materials Science, 2002, 33, 57-71.	1.1	57
50	Tuning hardness and fracture resistance of ZrN/Zr0.63Al0.37N nanoscale multilayers by stress-induced transformation toughening. Acta Materialia, 2015, 89, 22-31.	3.8	57
51	The effects of bias voltage and annealing on the microstructure and residual stress of arc-evaporated Cr–N coatings. Surface and Coatings Technology, 1999, 120-121, 272-276.	2.2	55
52	Thermomechanical properties of copper–carbon nanofibre composites prepared by spark plasma sintering and hot pressing. Composites Science and Technology, 2010, 70, 2263-2268.	3.8	53
53	Pressure and temperature effects on the decomposition of arc evaporated Ti0.6Al0.4N coatings in continuous turning. Surface and Coatings Technology, 2012, 209, 203-207.	2.2	52
54	Shape engineering boosts antibacterial activity of chitosan coated mesoporous silica nanoparticle doped with silver: a mechanistic investigation. Journal of Materials Chemistry B, 2016, 4, 3292-3304.	2.9	50

#	Article	IF	CITATIONS
55	Influence of plasma nitriding on fatigue strength and fracture of a B-Mn steel. Materials Science & Engineering A: Structural Materials: Properties, Microstructure and Processing, 1998, 242, 181-194.	2.6	49
56	Growth and characterization of TiN/SiN(001) superlattice films. Journal of Materials Research, 2007, 22, 3255-3264.	1.2	49
57	Load partitioning between single bulk grains in a two-phase duplex stainless steel during tensile loading. Acta Materialia, 2010, 58, 734-744.	3.8	49
58	Effect of laser hardening on the fatigue strength and fracture of a B–Mn steel. International Journal of Fatigue, 1998, 20, 389-398.	2.8	48
59	Vibrational free energy and phase stability of paramagnetic and antiferromagnetic CrN from <i>ab initio</i> molecular dynamics. Physical Review B, 2014, 89, .	1.1	46
60	Temperature-dependent elastic properties of Ti1â^' <i>x</i> Al <i>x</i> N alloys. Applied Physics Letters, 2015, 107, .	1.5	46
61	Microstructure–property relationships in arc-evaporated Cr–N coatings. Thin Solid Films, 2000, 377-378, 407-412.	0.8	44
62	Decomposition and phase transformation in TiCrAlN thin coatings. Journal of Vacuum Science and Technology A: Vacuum, Surfaces and Films, 2012, 30, .	0.9	44
63	Tuning the Shape of Mesoporous Silica Particles by Alterations in Parameter Space: From Rods to Platelets. Langmuir, 2013, 29, 13551-13561.	1.6	44
64	Growth and thermal stability of TiN/ZrAlN: Effect of internal interfaces. Acta Materialia, 2016, 121, 396-406.	3.8	44
65	Systematic ab initio investigation of the elastic modulus in quaternary transition metal nitride alloys and their coherent multilayers. Acta Materialia, 2017, 127, 124-132.	3.8	44
66	Deformation structures under indentations in TiN/NbN single-crystal multilayers deposited by magnetron sputtering at different bombarding ion energies. Philosophical Magazine A: Physics of Condensed Matter, Structure, Defects and Mechanical Properties, 2002, 82, 1983-1992.	0.8	41
67	Extended studies of degradation mechanisms in the refractory lining of a rotary kiln for iron ore pellet production. Journal of the European Ceramic Society, 2012, 32, 1519-1528.	2.8	41
68	Surface directed spinodal decomposition at TiAlN/TiN interfaces. Journal of Applied Physics, 2013, 113, .	1.1	41
69	High temperature phase evolution of Bolivian kaolinitic–illitic clays heated to 1250°C. Applied Clay Science, 2014, 101, 100-105.	2.6	41
70	Impact of nitrogen vacancies on the high temperature behavior of (Ti1â^'xAlx)Ny alloys. Acta Materialia, 2016, 119, 218-228.	3.8	41
71	The Reactivity of Ti2AlC and Ti3SiC2 with SiC Fibers and Powders up to Temperatures of 1550°C. Journal of the American Ceramic Society, 2011, 94, 1737-1743.	1.9	40
72	Phase-field modelling of spinodal decomposition in TiAlN including the effect of metal vacancies. Scripta Materialia, 2015, 95, 42-45.	2.6	40

#	Article	IF	CITATIONS
73	Mesoporous silica and carbon based catalysts for esterification and biodiesel fabrication—The effect of matrix surface composition and porosity. Applied Catalysis A: General, 2017, 533, 49-58.	2.2	40
74	Enhanced thermal stability and fracture toughness of TiAlN coatings by Cr, Nb and V-alloying. Surface and Coatings Technology, 2018, 342, 85-93.	2.2	40
75	Influence of synthesis temperature on morphology of SBA-16 mesoporous materials with a three-dimensional pore system. Microporous and Mesoporous Materials, 2010, 129, 106-111.	2.2	39
76	Nanofibrillated Celluloseâ€Based Electrolyte and Electrode for Paperâ€Based Supercapacitors. Advanced Sustainable Systems, 2018, 2, 1700121.	2.7	38
77	Deformation behaviour of a prestrained duplex stainless steel. Materials Science & Engineering A: Structural Materials: Properties, Microstructure and Processing, 2002, 337, 25-38.	2.6	37
78	Age hardening in arc-evaporated ZrAlN thin films. Scripta Materialia, 2010, 62, 739-741.	2.6	37
79	Propylsulfonic acid functionalized mesoporous silica catalysts for esterification of fatty acids. Journal of Molecular Catalysis A, 2015, 410, 253-259.	4.8	37
80	Residual Stresses in a Nickel-Based Superalloy Introduced by Turning. Materials Science Forum, 2002, 404-407, 173-178.	0.3	36
81	Annealing of Thermally Sprayed Ti2AlC Coatings. International Journal of Applied Ceramic Technology, 2011, 8, 74-84.	1.1	36
82	Microstructure evolution and age hardening in (Ti,Si)(C,N) thin films deposited by cathodic arc evaporation. Thin Solid Films, 2010, 519, 1397-1403.	0.8	35
83	Nanolabyrinthine ZrAlN thin films by self-organization of interwoven single-crystal cubic and hexagonal phases. APL Materials, 2013, 1, .	2.2	35
84	High pressure and high temperature stabilization of cubic AlN in Ti0.60Al0.40N. Journal of Applied Physics, 2013, 113, .	1.1	34
85	Targeted delivery of a novel anticancer compound anisomelic acid using chitosan-coated porous silica nanorods for enhancing the apoptotic effect. Biomaterials Science, 2015, 3, 103-111.	2.6	34
86	Comparison between slip-casting and uniaxial pressing for the fabrication of translucent yttria ceramics. Journal of Materials Science, 2008, 43, 2849-2856.	1.7	33
87	X-ray diffraction determination of residual stresses in functionally graded WC–Co composites. International Journal of Refractory Metals and Hard Materials, 2004, 22, 177-184.	1.7	32
88	Synthesis and characterization of large mesoporous silica SBA-15 sheets with ordered accessible 18Ânm pores. Materials Letters, 2009, 63, 2129-2131.	1.3	31
89	Thermal stability and mechanical properties of arc evaporated ZrN/ZrAlN multilayers. Thin Solid Films, 2010, 519, 694-699.	0.8	31
90	Anisotropy effects on microstructure and properties in decomposed arc evaporated Ti1-xAlxN coatings during metal cutting. Surface and Coatings Technology, 2013, 235, 181-185.	2.2	31

#	Article	IF	CITATIONS
91	Structure, deformation and fracture of arc evaporated Zr–Si–N hard films. Surface and Coatings Technology, 2014, 258, 1100-1107.	2.2	31
92	Microstructural characterization of alkali metal mediated high temperature reactions in mullite based refractories. Ceramics International, 2010, 36, 733-740.	2.3	30
93	High Si content TiSiN films with superior oxidation resistance. Surface and Coatings Technology, 2020, 398, 126087.	2.2	30
94	Intergranular strains and plastic deformation of an austenitic stainless steel. Materials Science & Engineering A: Structural Materials: Properties, Microstructure and Processing, 2002, 334, 215-222.	2.6	29
95	Growth of Gd2O3 nanoparticles inside mesoporous silica frameworks. Microporous and Mesoporous Materials, 2013, 168, 221-224.	2.2	29
96	Elastic strain evolution and ε-martensite formation in individual austenite grains during in situ loading of a metastable stainless steel. Materials Letters, 2008, 62, 338-340.	1.3	28
97	Self-organized anisotropic (Zr1â^'Si )N nanocomposites grown by reactive sputter deposition. Acta Materialia, 2015, 82, 179-189.	3.8	27
98	Exploring the high entropy alloy concept in (AlTiVNbCr)N. Thin Solid Films, 2017, 636, 346-352.	0.8	27
99	In situx-ray diffraction study ofC60polymerization at high pressure and temperature. Physical Review B, 2002, 66, .	1.1	26
100	Influence of chemical composition and deposition conditions on microstructure evolution during annealing of arc evaporated ZrAlN thin films. Journal of Vacuum Science and Technology A: Vacuum, Surfaces and Films, 2012, 30, .	0.9	26
101	The production of porous brick material from diatomaceous earth and Brazil nut shell ash. Construction and Building Materials, 2015, 98, 257-264.	3.2	26
102	Eutectic modification by ternary compound cluster formation in Al-Si alloys. Scientific Reports, 2019, 9, 5506.	1.6	26
103	Temperature-dependent elastic properties of binary and multicomponent high-entropy refractory carbides. Materials and Design, 2021, 204, 109634.	3.3	26
104	Comparison of relative permeability–fluid saturation–capillary pressure relations in the modelling of non-aqueous phase liquid infiltration in variably saturated, layered media. Advances in Water Resources, 2006, 29, 1705-1730.	1.7	24
105	Grinding-induced metallurgical alterations in the binder phase of WC-Co cemented carbides. Materials Characterization, 2017, 134, 302-310.	1.9	24
106	Effect of Drying and Dewatering on Yttria Precursors with Transient Morphology. Journal of the American Ceramic Society, 2006, 89, 3094-3100.	1.9	23
107	Wear behavior of ZrAIN coated cutting tools during turning. Surface and Coatings Technology, 2015, 282, 180-187.	2.2	23
108	Synthesis of a Cu-infiltrated Zr-doped SBA-15 catalyst for CO <sub>2</sub> hydrogenation into methanol and dimethyl ether. Physical Chemistry Chemical Physics, 2017, 19, 19139-19149.	1.3	23

#	Article	IF	CITATIONS
109	Phase Evaluation in <scp>Al<sub>2</sub>O<sub>3</sub></scp> Fiberâ€Reinforced <scp>Ti<sub>2</sub>AlC</scp> During Sintering in the 1300°C–1500°C Temperature Range. Journal of the American Ceramic Society, 2011, 94, 3327-3334.	1.9	22
110	Influence of Si content on phase stability and mechanical properties of TiAlSiN films grown by AlSi-HiPIMS/Ti-DCMS co-sputtering. Surface and Coatings Technology, 2021, 427, 127661.	2.2	22
111	Thermal treatment and phase formation in kaolinite and illite based clays from tropical regions of Bolivia. IOP Conference Series: Materials Science and Engineering, 2012, 31, 012017.	0.3	21
112	Growth of hard amorphous TiAlSiN thin films by cathodic arc evaporation. Surface and Coatings Technology, 2013, 235, 376-382.	2.2	21
113	Substrate surface finish effects on scratch resistance and failure mechanisms of TiN-coated hardmetals. Surface and Coatings Technology, 2015, 265, 174-184.	2.2	21
114	Thermal stability of wurtzite Zr1â^'xAlxN coatings studied by <i>in situ</i> high-energy x-ray diffraction during annealing. Journal of Applied Physics, 2015, 118, .	1.1	20
115	Impact of anharmonic effects on the phase stability, thermal transport, and electronic properties of AlN. Physical Review B, 2016, 94, .	1.1	20
116	Formation of block-copolymer-templated mesoporous silica. Journal of Colloid and Interface Science, 2018, 521, 183-189.	5.0	20
117	Near-Surface Deformation in an Alumina-Silicon Carbide-Whisker Composite due to Surface Machining. Journal of the American Ceramic Society, 1996, 79, 2134-2140.	1.9	19
118	Alternative method to precipitation techniques for synthesizing yttrium oxide nanopowder. Powder Technology, 2007, 177, 77-82.	2.1	19
119	Effect of heat treatment of carbon nanofibres on electroless copper deposition. Composites Science and Technology, 2010, 70, 2269-2275.	3.8	19
120	Characterization of worn Ti–Si cathodes used for reactive cathodic arc evaporation. Journal of Vacuum Science and Technology A: Vacuum, Surfaces and Films, 2010, 28, 347-353.	0.9	19
121	Ti–Si–C–N thin films grown by reactive arc evaporation from Ti <sub>3</sub> SiC <sub>2</sub> cathodes. Journal of Materials Research, 2011, 26, 874-881.	1.2	19
122	3D Microstructure Characterization and Analysis of Al-Si Foundry Alloys at Different Length Scales. Microscopy and Microanalysis, 2014, 20, 956-957.	0.2	19
123	Temperature induced superhard CrB 2 coatings with preferred (001) orientation deposited by DC magnetron sputtering technique. Surface and Coatings Technology, 2017, 322, 134-140.	2.2	19
124	Time evolution of the CO2 hydrogenation to fuels over Cu-Zr-SBA-15 catalysts. Journal of Catalysis, 2018, 362, 55-64.	3.1	19
125	Superhard and superelastic films of polymeric C60. Diamond and Related Materials, 2001, 10, 2044-2048.	1.8	18
126	Optimization of wear-resistant coating architectures using finite element analysis. Journal of Vacuum Science and Technology A: Vacuum, Surfaces and Films, 2003, 21, 332-339.	0.9	18

#	Article	IF	CITATIONS
127	Comparison of two different precipitation routes leading to Yb doped Y2O3 nano-particles. Journal of the European Ceramic Society, 2007, 27, 1991-1998.	2.8	18
128	Influence of Agglomeration on the Transparency of Yttria Ceramics. Journal of the American Ceramic Society, 2008, 91, 3380-3387.	1.9	18
129	Synthesis of homogeneously dispersed cobalt nanoparticles in the pores of functionalized SBA-15 silica. Powder Technology, 2012, 221, 359-364.	2.1	18
130	Blind deconvolution of time-of-flight mass spectra from atom probe tomography. Ultramicroscopy, 2013, 132, 60-64.	0.8	18
131	Solid state formation of Ti4AlN3 in cathodic arc deposited (Ti1â^'xAlx)Ny alloys. Acta Materialia, 2017, 129, 268-277.	3.8	18
132	Effect of nitrogen vacancies on the growth, dislocation structure, and decomposition of single crystal epitaxial (Ti1-xAlx)Ny thin films. Acta Materialia, 2021, 203, 116509.	3.8	18
133	Grain-to-Grain Stress Interactions in an Electrodeposited Iron Coating. Advanced Materials, 2005, 17, 1221-1226.	11.1	17
134	Synthesis and optical properties of Yb0.6Y1.4O3 transparent ceramics. Journal of Alloys and Compounds, 2008, 464, 407-411.	2.8	17
135	Growth and characterization of electroless deposited Cu films on carbon nanofibers. Surface and Coatings Technology, 2009, 203, 3459-3464.	2.2	17
136	Synthesis of hollow silica spheres SBA-16 with large-pore diameter. Materials Letters, 2011, 65, 1066-1068.	1.3	17
137	A new approach to account for fracture aperture variability when modeling solute transport in fracture networks. Water Resources Research, 2013, 49, 2241-2252.	1.7	17
138	Effects of nitrogen vacancies on phase stability and mechanical properties of arc deposited (Ti 0.52 Al) Tj ETQq0	0	Overlock 10 1
139	Enhanced thermal stability and mechanical properties of nitrogen deficient titanium aluminum nitride (Ti0.54Al0.46Ny) thin films by tuning the applied negative bias voltage. Journal of Applied Physics, 2017, 122, .	1.1	17
140	Impact of the morphological and chemical properties of copper-zirconium-SBA-15 catalysts on the conversion and selectivity in carbon dioxide hydrogenation. Journal of Colloid and Interface Science, 2019, 546, 163-173.	5.0	17
141	Microstructural influence of the thermal behavior of arc deposited TiAlN coatings with high aluminum content. Journal of Alloys and Compounds, 2021, 854, 157205.	2.8	17
142	Morphology effects on electrocatalysis of anodic water splitting on nickel (II) oxide. Microporous and Mesoporous Materials, 2022, 333, 111734.	2.2	17
143	Degradation of Refractory Bricks Used as Thermal Insulation in Rotary Kilns for Iron Ore Pellet Production. International Journal of Applied Ceramic Technology, 2009, 6, 717-726.	1.1	16
144	On the Stability of Mg Nanograins to Coarsening after Repeated Melting. Nano Letters, 2009, 9, 3082-3086.	4.5	16

#	Article	IF	CITATIONS
145	Phase transformations in nanocomposite ZrAlN thin films during annealing. Journal of Materials Research, 2012, 27, 1716-1724.	1.2	16
146	Microstructural and Chemical Analysis of Agl Coatings Used as a Solid Lubricant in Electrical Sliding Contacts. Tribology Letters, 2012, 46, 187-193.	1.2	16
147	Influence of Ti–Si cathode grain size on the cathodic arc process and resulting Ti–Si–N coatings. Surface and Coatings Technology, 2013, 235, 637-647.	2.2	16
148	Single-pot synthesis of ordered mesoporous silica films with unique controllable morphology. Journal of Colloid and Interface Science, 2014, 413, 1-7.	5.0	16
149	Mechanical strength of ground WC-Co cemented carbides after coating deposition. Materials Science & Engineering A: Structural Materials: Properties, Microstructure and Processing, 2017, 689, 72-77.	2.6	16
150	Regional channelized transport in fractured media with matrix diffusion and linear sorption. Water Resources Research, 2008, 44, .	1.7	15
151	Morphology influence of the oxidation kinetics of carbon nanofibers. Corrosion Science, 2009, 51, 926-930.	3.0	15
152	Arc deposition of Ti–Si–C–N thin films from binary and ternary cathodes — Comparing sources of C. Surface and Coatings Technology, 2012, 213, 145-154.	2.2	15
153	Improved metal cutting performance with bias-modulated textured Ti0.50Al0.50N multilayers. Surface and Coatings Technology, 2014, 257, 102-107.	2.2	15
154	Growth, structure, and mechanical properties of transition metal carbide superlattices. Journal of Materials Research, 2001, 16, 1301-1310.	1.2	14
155	Hardness profile measurements in functionally graded WC–Co composites. Materials Science & Engineering A: Structural Materials: Properties, Microstructure and Processing, 2004, 382, 141-149.	2.6	14
156	Reverse Martensitic Transformation and Resulting Microstructure in a Cold Rolled Metastable Austenitic Stainless Steel. Steel Research International, 2008, 79, 433-439.	1.0	13
157	High temperature phase decomposition in TixZryAlzN. AIP Advances, 2014, 4, .	0.6	13
158	Contact damage resistance of TiN-coated hardmetals: Beneficial effects associated with substrate grinding. Surface and Coatings Technology, 2015, 275, 133-141.	2.2	13
159	Non-equilibrium vacancy formation energies in metastable alloys — A case study ofÂTi0.5Al0.5N. Materials and Design, 2017, 114, 484-493.	3.3	13
160	Residual stress in clinched joints of metals. Applied Physics A: Materials Science and Processing, 2002, 74, s1440-s1442.	1.1	12
161	Microstructure and thermal stability of arc-evaporated Cr–C–N coatings. Philosophical Magazine, 2004, 84, 611-630.	0.7	12
162	Dislocation structure and microstrain evolution during spinodal decomposition of reactive magnetron sputtered heteroepixatial c-(Ti0.37,Al0.63)N/c-TiN films grown on MgO(001) and (111) substrates. Journal of Applied Physics, 2019, 125, .	1,1	12

#	Article	IF	CITATIONS
163	Spectroscopic investigation on the near-substrate plasma characteristics of chromium HiPIMS in low density discharge mode. Plasma Sources Science and Technology, 2020, 29, 015013. Strength, transformation toughening, and tracture dynamics of Processalt-structure crimil:math	1.3	12
164	xmlns:mml="http://www.w3.org/1998/Math/MathML"> <mml:mrow><mml:mi mathvariant="normal"&gt;T<mml:msub><mml:mi mathvariant="normal"&gt;i<mml:mrow><mml:mn>1</mml:mn><mml:mo>â^²</mml:mo><mml:mi>xmathvariant="normal"&gt;A</mml:mi><mml:msub><mml:mi mathvariant="normal"&gt;I&lt;<mml:mi><td>ıml<b>:m</b>∳ <td>nmluznrow&gt;</td></td></mml:mi></mml:mi </mml:msub></mml:mrow></mml:mi </mml:msub></mml:mi </mml:mrow>	ıml <b>:m</b> ∳ <td>nmluznrow&gt;</td>	nmluznrow>
165	mathyariant="normal">(Mininim Commitme Commitme Commitme Commitme Commitme Commitme mathyariant="normal" > N From well-test data to input to stochastic continuum models: effect of the variable support scale of the hydraulic data. Hydrogeology Journal, 2006, 14, 1409-1422.	0.9	11
166	Auto-organizing ZrAlN/ZrAlTiN/TiN multilayers. Thin Solid Films, 2012, 520, 6451-6454.	0.8	11
167	Industry-relevant magnetron sputtering and cathodic arc ultra-high vacuum deposition system for <i>in situ</i> x-ray diffraction studies of thin film growth using high energy synchrotron radiation. Review of Scientific Instruments, 2015, 86, 095113.	0.6	11
168	Morphology and microstructure evolution of Ti-50 at.% Al cathodes during cathodic arc deposition of Ti-Al-N coatings. Journal of Applied Physics, 2017, 121, 245309.	1.1	11
169	The effect of nitrogen vacancies on initial wear in arc deposited (Ti0.52,Al0.48)Ny, (y < 1) coatings during machining. Surface and Coatings Technology, 2019, 358, 452-460.	2.2	11
170	Influence of pulsed-substrate bias duty cycle on the microstructure and defects of cathodic arc-deposited Ti1-xAlxN coatings. Surface and Coatings Technology, 2021, 419, 127295.	2.2	11
171	Thermally induced structural evolution and age-hardening of polycrystalline V1–xMoxN (xÂâ‰^Â0.4) thin films. Surface and Coatings Technology, 2021, 405, 126723.	2.2	11
172	Microstructure evolution of Ti3SiC2 compound cathodes during reactive cathodic arc evaporation. Journal of Vacuum Science and Technology A: Vacuum, Surfaces and Films, 2011, 29, 031601.	0.9	10
173	Coherency strain engineered decomposition of unstable multilayer alloys for improved thermal stability. Journal of Applied Physics, 2013, 114, .	1.1	10
174	Anomalous epitaxial stability of (001) interfaces in ZrN/SiNx multilayers. APL Materials, 2014, 2, 046106.	2.2	10
175	Self-organized nanostructuring in Zr0.69Al0.31N thin films studied by atom probe tomography. Thin Solid Films, 2016, 615, 233-238.	0.8	10
176	Coherency effects on the mixing thermodynamics of cubic <mml:math xmlns:mml="http://www.w3.org/1998/Math/MathML"&gt;<mml:mrow><mml:msub><mml:mi>Ti</mml:mi><mml:r mathvariant="normal"&gt;N<mml:mo>/</mml:mo><mml:mi>TiN</mml:mi></mml:r </mml:msub></mml:mrow> multilayers. Physical Review B, 2016, 93, .</mml:math 	nrowş <mr <td>nl:mŋ&gt;1h&gt;(001)</td></mr 	nl:mŋ>1h>(001)
177	Influence of microstructure and mechanical properties on the tribological behavior of reactive arc deposited Zr-Si-N coatings at room and high temperature. Surface and Coatings Technology, 2016, 304, 393-400.	2.2	10
178	Characterization of DLC coatings over nitrided stainless steel with and without nitriding pre-treatment using annealing cycles. Journal of Materials Research and Technology, 2019, 8, 1653-1662.	2.6	10
179	A shelf-life study of silica- and carbon-based mesoporous materials. Journal of Industrial and Engineering Chemistry, 2021, 101, 205-213.	2.9	10
180	Electrochemically deposited nickel membranes; process–microstructure–property relationships. Surface and Coatings Technology, 2003, 172, 79-89.	2.2	9

#	Article	IF	CITATIONS
181	Special quasirandom structure method in application for advanced properties of alloys: A study on Ti 0.5 Al 0.5 N and TiN/Ti 0.5 Al 0.5 N multilayer. Computational Materials Science, 2015, 103, 194-199.	1.4	9
182	Influence of substrate microstructure and surface finish on cracking and delamination response of TiN-coated cemented carbides. Wear, 2016, 352-353, 102-111.	1.5	9
183	Discharge state transition and cathode fall thickness evolution during chromium HiPIMS discharge. Physics of Plasmas, 2017, 24, .	0.7	9
184	Effects of decomposition route and microstructure on h-AlN formation rate in TiCrAlN alloys. Journal of Alloys and Compounds, 2017, 691, 1024-1032.	2.8	9
185	Growth and Functionalization of Particle-Based Mesoporous Silica Films and Their Usage in Catalysis. Nanomaterials, 2019, 9, 562.	1.9	9
186	Thermal degradation of TiN and TiAlN coatings during rapid laser treatment. Surface and Coatings Technology, 2021, 422, 127517.	2.2	9
187	Deformation structures under indentations in TiN/NbN single-crystal multilayers deposited by magnetron sputtering at different bombarding ion energies. , 0, .		9
188	RHEED studies during growth of TiN/SiNx/TiN trilayers on MgO(001). Surface Science, 2007, 601, 2352-2356.	0.8	8
189	Thermal and mechanical stability of wurtzite-ZrAlN/cubic-TiN and wurtzite-ZrAlN/cubic-ZrN multilayers. Surface and Coatings Technology, 2017, 324, 328-337.	2.2	8
190	Growth and high temperature decomposition of epitaxial metastable wurtzite (Ti1-x,Alx)N(0001) thin films. Thin Solid Films, 2019, 688, 137414.	0.8	8
191	Effect of work function and cohesive energy of the constituent phases of Ti-50â€ <sup>-</sup> at.% Al cathode during arc deposition of Ti-Al-N coatings. Surface and Coatings Technology, 2019, 357, 393-401.	2.2	8
192	3D FIB/FESEM tomography of grinding-induced damage in WC-Co cemented carbides. Procedia CIRP, 2020, 87, 385-390.	1.0	8
193	Synthesis of nanocrystalline yttria through in-situ sulphated-combustion technique. Journal of the Ceramic Society of Japan, 2009, 117, 1065-1068.	0.5	7
194	High temperature thermodynamics of spinodal decomposition in arc deposited TixNbyAlzN coatings. Materials and Design, 2018, 150, 165-170.	3.3	7
195	Nanostructuring and coherency strain in multicomponent hard coatings. APL Materials, 2014, 2, 116104.	2.2	6
196	The Effect of Cathodic Arc Guiding Magnetic Field on the Growth of (Ti0.36Al0.64)N Coatings. Coatings, 2019, 9, 660.	1.2	6
197	Decomposition routes and strain evolution in arc deposited TiZrAlN coatings. Journal of Alloys and Compounds, 2019, 779, 261-269.	2.8	6
198	Residual Stress Distributions around Clinched Joints. Materials Science Forum, 2002, 404-407, 617-622.	0.3	5

#	Article	IF	CITATIONS
199	Mesoporous silica templated zirconia nanoparticles. Journal of Nanoparticle Research, 2011, 13, 2743-2748.	0.8	5
200	Low temperature nanocasting of hematite nanoparticles using mesoporous silica molds. Powder Technology, 2012, 217, 269-273.	2.1	5
201	Thermal expansion of quaternary nitride coatings. Journal of Physics Condensed Matter, 2018, 30, 135901.	0.7	5
202	Crater wear mechanism of TiAlN coatings during high-speed metal turning. Wear, 2021, 484-485, 204016.	1.5	5
203	Anisotropic High Cycle Fatigue Behaviour of Duplex Stainless Steels: Influence of Microstresses. International Journal of Materials Research, 2002, 93, 7-11.	0.8	5
204	Sintering, microstructural and mechanical characterization of combustion synthesized Y2O3 and Yb3+-Y2O3. Journal of the Ceramic Society of Japan, 2009, 117, 1258-1262.	0.5	4
205	Silica SBA-15 Template Assisted Synthesis of Ultrasmall and Homogeneously Sized Copper Nanoparticles. Journal of Nanoscience and Nanotechnology, 2011, 11, 3493-3498.	0.9	4
206	Growth of single crystalline dendritic Li2SiO3 arrays from LiNO3 and mesoporous SiO2. Journal of Solid State Chemistry, 2011, 184, 1735-1739.	1.4	4
207	Thermally Induced Surface Integrity Changes of Ground WC-Co Hardmetals. Procedia CIRP, 2016, 45, 91-94.	1.0	4
208	Effect of varying N <sub>2</sub> pressure on DC arc plasma properties and microstructure of TiAlN coatings. Plasma Sources Science and Technology, 2020, 29, 095015.	1.3	4
209	Characterisation of residual stress distribution in clinching joints of carbon steel by diffraction methods. Materials Science and Technology, 2003, 19, 336-342.	0.8	3
210	Residual Stress Analysis in Both As-Deposited and Annealed CrN Coatings. Materials Science Forum, 2005, 490-491, 643-648.	0.3	3
211	Effects of the cathode grain size and substrate fixture movement on the evolution of arc evaporated Cr-cathodes and Cr-N coating synthesis. Journal of Vacuum Science and Technology A: Vacuum, Surfaces and Films, 2014, 32, 021515.	0.9	3
212	A custom built lathe designed for <i>in operando</i> high-energy x-ray studies at industrially relevant cutting parameters. Review of Scientific Instruments, 2019, 90, .	0.6	3
213	xmlns:mml="http://www.w3.org/1998/Math/Math/Math/Math/Math/Math/Math/Math	ml <b>:ma</b> > <td>nm<b>b</b>mrow&gt;&lt;</td>	nm <b>b</b> mrow><
214	Evolution of Residual Strains in Metastable Austenitic Stainless Steels and the Accompanying Strain Induced Martensitic Transformation. Materials Science Forum, 2006, 524-525, 821-826.	0.3	2
215	Residual Stress Evolution during Decomposition of Ti <sub>(1-x)</sub> Al <sub>(x)</sub> N Coatings Using High-Energy X-Rays. Materials Science Forum, 2006, 524-525, 619-624.	0.3	2
216	Synthesis of Ti3SiC2 by Reaction of TiC and Si Powders. Ceramic Engineering and Science Proceedings, 0, , 21-30.	0.1	2

#	Article	IF	CITATIONS
217	Preparation and firing of a TiC/Si powder mixture. IOP Conference Series: Materials Science and Engineering, 2009, 5, 012016.	0.3	2
218	Implementation of advanced characterisation techniques for assessment of grinding effects on the surface integrity of WC–Co cemented carbides. Powder Metallurgy, 2018, 61, 100-105.	0.9	2
219	Phase Selective Sample Preparation of Al-Si alloys for Atom Probe Tomography. Praktische Metallographie/Practical Metallography, 2019, 56, 76-90.	0.1	2
220	Internal Stress in an Alumina/Silicon Carbide Whisker Composite. Advances in X-ray Analysis, 1995, 39, 391-403.	0.0	1
221	Free Standing AlN Single Crystal Grown on Pre-Patterned and <i>In Situ</i> Patterned 4H-SiC Substrates. Materials Science Forum, 0, 645-648, 1187-1190.	0.3	1
222	Internal Stress in an Alumina/Silicon Carbide Whisker Composite. , 1997, , 391-403.		1
223	Micro- and Macrostress Evolution in a Duplex Stainless Steel during Uniaxial Loading. Materials Science Forum, 2000, 347-349, 603-608.	0.3	0
224	Determination of Grain-Orientation-Dependent Stress in Coatings. Solid State Phenomena, 2005, 105, 107-112.	0.3	0
225	Complex 3D nanocoral like structures formed by copper nanoparticle aggregation on nanostructured zinc oxide rods. Materials Letters, 2016, 184, 127-130.	1.3	0
226	Synthesis and Phase Development in the Cr-Al-N System. Ceramic Engineering and Science Proceedings, 0, , 1-12.	0.1	0
227	Carbon Based Coatings Deposited on Nitrided Stainless Steel: Study of Thermal Degradation. Minerals, Metals and Materials Series, 2017 57-66	0.3	0